

Metal veins in the Kernouvé (H6 S1) chondrite: Evidence for pre- or syn-metamorphic shear deformation

Jon M. Friedrich^{a,b,*}, Alex Ruzicka^c, Mark L. Rivers^d, Denton S. Ebel^b,
James O. Thostenson^e, Rebecca A. Rudolph^{e,1}

^a Department of Chemistry, Fordham University, Bronx, NY 10458, United States

^b Department of Earth and Planetary Sciences, American Museum of Natural History, New York, NY 10024, United States

^c Cascadia Meteorite Laboratory, Portland State University, Department of Geology, Portland, OR 97207-0751, United States

^d Consortium for Advanced Radiation Sources, University of Chicago, Argonne, IL 60439, United States

^e Microscopy and Imaging Facility, American Museum of Natural History, New York, NY 10024, United States

Available online 1 February 2013

Abstract

Kernouvé is an H6 chondrite that experienced a very small degree of late stage shock loading (S1). However, Kernouvé contains Fe–Ni metal vein-like structures, whose formation have been attributed to an early impact event. To establish the formation conditions of metal veins in Kernouvé, we examined the three dimensional (3D) arrangement of metal vein-like structures and typical metal grains in two samples of Kernouvé with X-ray microtomography (μ CT) at resolutions of $\sim 11 \mu\text{m}/\text{voxel}$. We additionally investigated the 3D structure of the porosity present in Kernouvé using μ CT at two different resolutions (~ 3 and $\sim 11 \mu\text{m}/\text{voxel}$). These data and optical microscopy support the hypothesis that Kernouvé has experienced little post-metamorphic shock. However, the moderate 5.8 vol.% porosity of Kernouvé is in the form of intergranular voids rather than cracks, which indicates any cracking that may have existed in the relatively brittle silicate grains was annealed. We estimate that 70–80% of the primordial porosity in Kernouvé was removed by impact-related compaction. Moreover, we found no collective orientation of metal grains, so high metamorphic temperatures following compaction erased any common orientation of metal grains due to compaction. We propose that the metal vein structures can be explained as a pre- or syn-metamorphic shock-induced process, which we infer was primarily shear deformation, with some uniaxial compaction also occurring. The coarse metal veins probably formed by accumulation of ductile metal grains along shear zones, a process that would have been facilitated by having an already warm H chondrite parent body when shock occurred (i.e., syn-metamorphic shock). The complexity of shape, including numerous tendrils expanding from the primary structure, of the veins in Kernouvé is likely due to the coalescence of metal by metamorphic growth after the shear event. The metal veins in Kernouvé thus appear to record evidence for early, shock-induced metal mobilization and the maximum shock pressure experienced by Kernouvé may have been ≤ 21 GPa. Our study suggests that collision-induced segregation of metal occurred at an early stage in low-gravity planetesimals, consistent with the idea that this process could have been important for the differentiation of such objects.

© 2013 Elsevier Ltd. All rights reserved.

1. INTRODUCTION

Throughout the history of our solar system, impacts have been an inescapable part of the dynamic evolution of asteroids. The effects of these impacts can be found in the meteorites which have been delivered to Earth-crossing orbits and later collected. The primary quantifiable effects within meteorites include textural evidence for shock and

* Corresponding author at: Department of Chemistry, Fordham University, Bronx, NY 10458, United States. Tel.: +1 718 817 4446; fax: +1 718 817 4432.

E-mail address: friedrich@fordham.edu (J.M. Friedrich).

¹ Present address: GE Inspection Technologies, 50 Industrial Park Road, Lewistown, PA 17044, United States.

radiometric evidence of the heating which, depending on a rock's specific provenance, can accompany the impacts. The majority of ordinary chondrites, the most abundant type of meteorite on the Earth, contain some evidence of shock loading. However, occasionally chondrites appear to have largely escaped the effects of intense, late stage (significantly post metamorphic) shock events. They are classified as S1, the lowest shock stage, that experienced peak transient shock pressures <5–10 GPa (Stöffler et al., 1991), and show no obvious signs of later stage heating which would accompany impact processes. One of the best examples of a weakly shocked meteorite is the Kernouvé (H6 S1) ordinary chondrite. It is widely known to exhibit few traditional signs of late stage shock loading (Stöffler et al., 1991; Schmitt, 2000; Reisener and Goldstein, 2003; Rubin, 2004), and it has a very old ^{39}Ar – ^{40}Ar age of 4.46 Ga with no signs of heating past that time (Turner et al., 1978). Kernouvé shows systematic changes in closure ages for different chronometer systems, consistent with slow cooling following thermal metamorphism, suggesting that it was not disturbed by shock reheating after metamorphism (Trieloff et al., 2003; Kleine et al., 2008).

Although weakly shocked, an intriguing aspect of Kernouvé is the presence of large, cm-scale, Fe–Ni metal veins. Metallic veins in ordinary chondrites, like those found by petrographic thin section and hand specimen inspection of Kernouvé, have often been attributed to impact or shock processes on the parent body (Turner et al., 1978; Michel-Lévy, 1981; Hutson, 1989; Rubin, 1992, 2003, 2004; Leroux et al., 1996; Hutchison et al., 2001). Although Kernouvé does contain metal veins, these are not the silicate-rich “opaque” shock veins of Stöffler et al. (1991), i.e. they are not unambiguous indicators of shock. But this leaves a conundrum: how can one have impact-induced metallic veins within a sample that exhibits few traditional signs of shock loading? Both Hutson (1989) and later Hutchison et al. (2001) suggested that the vein formation occurred early in the history of the H chondrite parent body, prior to thermal metamorphism.

Here, we investigate the nature of the Fe–Ni metal vein formation process in Kernouvé. We use X-ray microtomography to examine the nature of the porosity within Kernouvé, which is known to give information on the impact history of ordinary chondrites (Friedrich et al., 2008a,b; Friedrich and Rivers, 2013). We can also examine the degree of compaction that Kernouvé experienced to further constrain its late stage shock history. Finally we examine the three dimensional (3D) structure of the veins in two samples of Kernouvé to examine the hypothesis that Kernouvé experienced a pre-metamorphic impact event. From this evidence, we show that shear deformation during an early impact event is the most likely scenario for the formation of metal veins in Kernouvé. This has implications for the dynamic evolution of small bodies in the solar system, as well as for core-formation processes on differentiated asteroids. Shear deformation can facilitate metal–silicate segregation by differentiating metal and silicates through either the concentration of metal between silicates during plastic flow (Bruhn et al., 2000; Groebner and Kohlstedt, 2006; Hustoft and Kohlstedt, 2006) or metal concentration

by localization within the cracks of brittle silicate grains (Rushmer and Petford, 2011).

2. SAMPLES AND METHODS

2.1. μCT imaging and petrographic analysis

Sample details are shown in Table 1. Two larger samples of Kernouvé (Sample 1, AMNH 470 subsample; and Sample 2, USNM 359 subsample) were examined with μCT . To better establish the shock history and nature of porosity in Kernouvé, we also examined three smaller chips of AMNH 470 (chips 1–3, see Table 1) with the same technique, but at a higher resolution.

Sample 1 was imaged at a resolution of 11.2 $\mu\text{m}/\text{voxel}$ (a voxel is a 3D volume element, akin to a 2D pixel) at the American Museum of Natural History with a GE phoenix v|tome|x s240 μCT system. Operating with a polychromatic X-ray tube at 80 μA and 135 keV, a 0.1 mm Cu filter was placed between the X-ray tube and sample to reduce imaging artifacts such as beam hardening. Sample 2 was imaged at a resolution of 11.9 $\mu\text{m}/\text{voxel}$ with monochromatic 50 keV X-rays using the 13-BMD beamline located at the Advanced Photon Source (APS) of the Argonne National Laboratory. These resolutions are known to be adequate for observing the morphology and size distribution of metal and sulfide grains in ordinary and other chondrites as well as examining porosity structures in partially compacted samples (Ebel et al., 2008; Friedrich et al., 2008a,b; Sasso et al., 2009; Beitz et al., 2013). From the 3D datasets, features can be visibly identified and digitally isolated for quantitative examination, and 2D slices (tomograms) can be extracted.

Kernouvé chips 1–3 were imaged at a resolution of 2.74 $\mu\text{m}/\text{voxel}$ with 40 keV monochromatic X-rays at the same APS beamline as above. Imaging ordinary chondrites at this resolution has been shown (Friedrich and Rivers, 2013) to be sufficient to image the total known porosity contained within them and to give porosity results comparable with ideal gas pycnometry (e.g., Macke, 2010). This data is useful for establishing the impact history of a rock (Friedrich and Rivers, 2013).

We examined two petrographic thin sections of Kernouvé (USNM 1054-1 and a sample derived from USNM 359 that was ultimately used for separate TEM study) and confirmed its classification as shock stage S1 in the scheme of Stöffler et al. (1991). This was accomplished by optical light microscopy of olivine grains using the criteria of Jamsja and Ruzicka (2010), based on the works of Stöffler et al. (1991), Schmitt and Stöffler (1995), and Schmitt (2000). The technique of Jamsja and Ruzicka assigns a shock stage to each suitable grain. Based on these observations, 74 olivine grains (89.2%) in Kernouvé conformed to shock stage S1, seven grains (8.4%) to S2, one grain each (1.2%) to S3 and S6, and no grains to S4 and S5. By the convention established by Stöffler et al. (1991) whereby the overall shock stage corresponds to the highest level shown by at least 25% of the grains, Kernouvé is clearly shock stage S1.

Table 1

Sample information, data collection details, and X-ray microtomography derived physical and compositional properties of five Kernouvé (H6 S1) chondrite samples.

Sample	Mass (mg)	μ CT resolution ($\mu\text{m}/\text{voxel}$)	Volume imaged (mm^3)	Bulk density (g/cm^3)	Porosity (vol.%) ^a	Metal (vol.%)	Sulfide (vol.%)
Sample 1 (AMNH 470)	4740	11.21	519 ^b	–	3.46	6.71	4.62
Sample 2 (USNM 359)	735.7	11.88	209	3.52	5.31	6.86	4.61
Chip 1 (AMNH 470)	37.65	2.74	10.43	3.61	5.94	6.71	2.97
Chip 2 (AMNH 470)	33.42	2.74	9.55	3.50	4.81	7.75	3.98
Chip 3 (AMNH 470)	22.11	2.74	6.09	3.63	6.57	10.18	3.61

^a μ CT visible porosity only.

^b The entire volume of Kernouvé Sample 1 was not imaged.

2.2. Digital 3D methods

Digital data extraction and visualization was accomplished with the software BLOB3D (Ketcham, 2005) and ImageJ, an open source software package. With BLOB3D, we are able to quantify the abundance of porosity and other phases in our samples through their digital isolation in 3D space. These separated components can then be projected using ImageJ. Friedrich et al. (2008a) demonstrated that the errors involved with quantifying each phase in chondrites with μ CT and digital data extraction are $\leq 6\%$. Metal vein structures were easily distinguished from the smaller, more typical, isolated H chondrite metal grains because of their large size and completely interconnected nature.

Three-dimensional quantification of the petrofabric within Kernouvé was accomplished by methods analogous to Friedrich et al. (2008a). In short, the metal grains within a sample are digitally isolated and best-fit ellipsoids are drawn around each. Using a variation of the orientation tensor method, the natural logarithm of the ratio of major over minor eigenvalues of the ellipsoids are computed to yield a strength factor C (Woodcock, 1977; Woodcock and Naylor, 1983). This is similar to but more general than the vector mean (or more specifically, resultant percentage) degree of preferred orientation ($R\%$) that was used in Friedrich et al. (2008a); however, the resulting graphical data appear identical for these samples. For this work, the higher the strength factor C , the greater the common orientation of the metal grains in the sample and the greater the compaction/shock loading apparent in the material volume under investigation.

3. RESULTS

We first use our data to establish the late stage impact history of Kernouvé. We will examine the porosity, degree of metal grain orientation, and petrographic observations. We will then examine the nature of the metallic veins and other metal phases within Kernouvé.

3.1. General observations

Typical tomograms, or 2D slices, from the greater 3D datasets of Samples 2 and 1 are shown in Figs. 1 and 2. In these, different mineralogical phases and porosity are identifiable and can be digitally isolated. Our high-resolution data for the small chips clearly show the presence of intergranular porosity that is comparable to the size of larger metal and sulfide grains (Fig. 1). Our data for the larger AMNH and USNM samples also clearly show the presence of metal veins that largely cross-cut the volumes of these samples (Fig. 2). These metal veins appear to be locally discontinuous in the tomograms (Fig. 2) but connect in the third dimension (see Electronic Annexes EA-1 and EA-2). No sulfide veins were found.

3.2. Fe–Ni metal and sulfide abundance and structure

The digital extraction techniques described in Section 2.2 allow the quantity of Fe–Ni metal present in our μ CT volumes to be quantified with accurate results (e.g., Friedrich et al., 2008a). Using the H chondrite fall data of Jarosewich (1990) and using a reasonable density for chondritic Fe–Ni metal, H chondrites possess a total metal volume of 7.3 ± 0.7 vol.% (mean and 1σ standard deviation). Our larger samples, including the metal veins, have total metal volumes of 6.71 and 6.86 vol.% (Table 1). Our smaller chips possess more deviation, a range of 6.71–10.18 vol.%, which bracket the values of the larger and therefore more representative samples. Using the total amount of metal within a sample as an indicator, our larger Kernouvé samples well represent a typical H chondrite. The same is true for sulfide abundance. Also, when the large metal veins are excluded from consideration, both metal and sulfide grain size distributions are consistent with previous size distributions for equilibrated H chondrites investigated by our group (Sasso et al., 2009). So overall, we find that the total metal volume (typical metal grains and vein metal in the larger samples) in our Kernouvé samples and chips is typical of H chondrites.

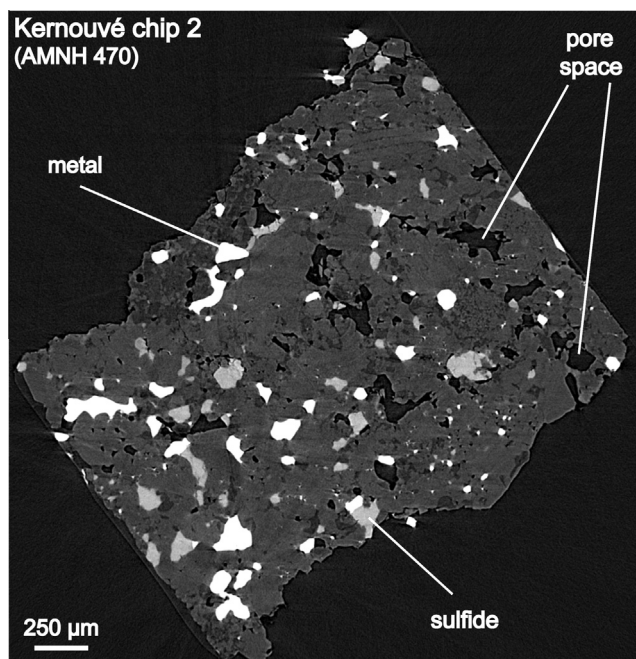


Fig. 1. A typical tomographic “slice” of chip 2 of the Kernouvé H chondrite collected at a resolution of 2.74 μm/voxel. Table 1 contains additional sample and data collection details. Higher mean atomic weight materials are indicated by brighter grayscale values. The (brightest) Fe–Ni metal grains and moderate grey FeS can easily be identified in between the darker silicate material. Black porosity or void spaces among the silicate minerals can also easily be visually distinguished. The 5.8 vol.% porosity in Kernouvé is present as intragranular voids rather than as μm-sized cracks.

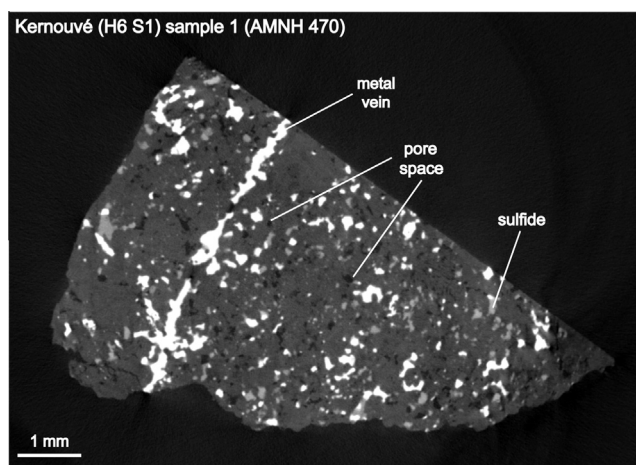


Fig. 2. A typical tomographic “slice” of Sample 1 of Kernouvé collected at a resolution of 11.2 μm/voxel. See Table 1 for additional sample and data collection details. The metal vein visible here crosscuts the entire sample. Note that the metal in the vein is not associated with FeS. This figure shows an orthogonal cross section (looking down from the top of the figure – note the positions of the cut surfaces) of the lower metal vein structure shown in Fig. 4.

We examined the orientation of the metal grains within Kernouvé. Fig. 3 shows that metal grains in Kernouvé do not possess significant preferred orientation, and have one of the lowest degrees of preferred orientation of any chondrite (Fig. 3). Although not shown, sulfide grains in Kernouvé also lack obvious preferred orientation. However, among the entire suite of samples we have examined, there is a general correlation between shock stage and degree of preferred orientation of metal grains (Fig. 3), consistent

with the idea that metal grains in chondrites became aligned during shock: such preferred orientation of metal and chondrules in chondrites has been interpreted to be the result of shock compaction (Friedrich et al., 2008a and references therein), and has been experimentally reproduced by shock loading (Nakamura et al., 2000). The μCT data for Kernouvé are consistent with optical petrography and suggest that the meteorite was not significantly shock compacted.

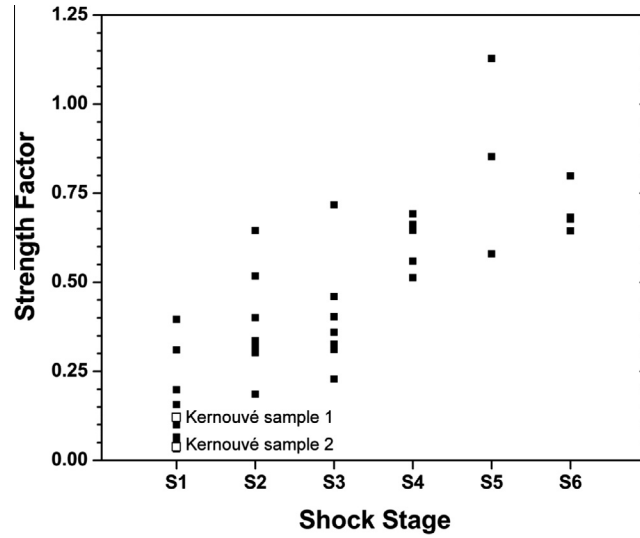


Fig. 3. Degree of preferred orientation of metal grains (given by the strength factor C , see Section 2.2) versus shock stage in equilibrated ordinary chondrites. Kernouvé has little common orientation of metal grains at present. Data here incorporated LL, L, and H chondrites, expanding the scheme from Friedrich et al. (2008a), which investigated only L chondrites. In this plot we have excluded the data for Leonovka due to a questionable shock state assignment – the thin section used for this sample in the earlier work was an older, glass-covered section which yielded suspicious and inconsistent results (see Friedrich et al., 2008a).

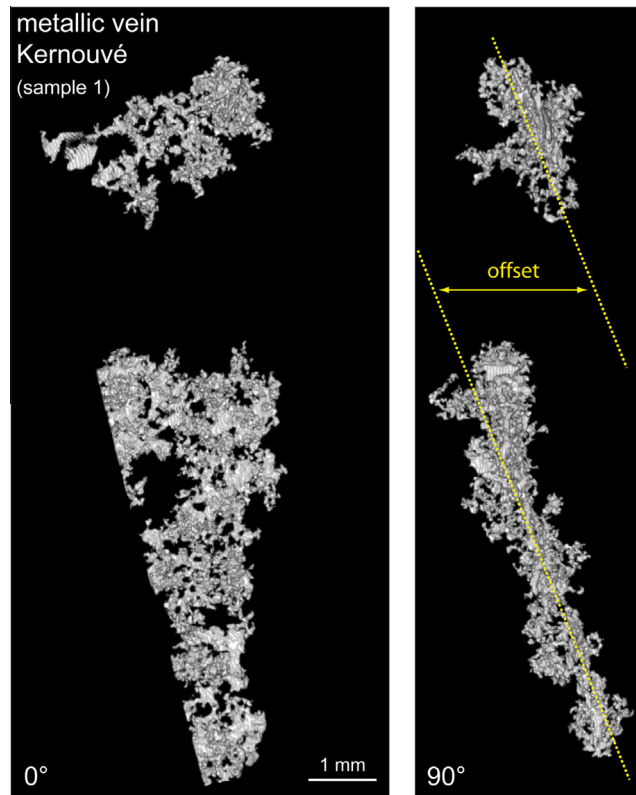


Fig. 4. 3D visualization of metal vein structure in Kernouvé (AMNH 470), consisting of two separate metal structures that trend in the same direction but are offset. Views are rotated 90° on a vertical rotation axis; a “face on” view is shown at left and an “edge on” view at right. The complexity of shape and degree of interconnectivity suggests a pre- or syn-metamorphic origin for the metallic vein structures. A cut surface occurs at the left side of the vein when seen in the 0° rotation view. A 3D rotating view of this figure can be found as EA-1.

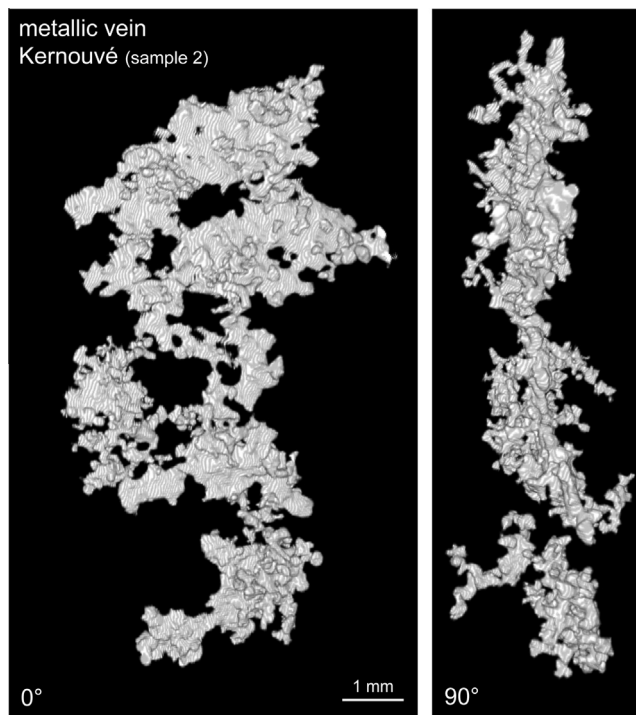


Fig. 5. 3D visualization of a metal vein structure in Kernouvé (USNM 359) consisting of two separate metal grains. Views are rotated 90° on a vertical rotation axis; a “face-on” view is shown at left and an “edge-on” view at right. As with the vein in Sample 1, the metal has complexity of shape and a high degree of interconnectivity. Tendrils of metal extend into the host meteorite away from the vein. A 3D rotating view of this figure can be found as [EA-2](#).

The 3D structure of metal veins in our Kernouvé samples are shown in [Figs. 4 and 5](#) (also see [Electronic Annexes EA-1 and EA-2](#)). The vein structures are each completely bounded by the tomographic volumes, i.e. entire vein structures are contained within our respective tomography stacks. Each vein has a striking complexity of shape: the veins are actually contiguous vein-like sheets with added tendrils of metal material adhering. In 2D, these tendrils appear as scalloped protrusions.

The vein in Sample 1 is discontinuous with the two portions appearing to be offset, but parallel in overall direction. Sample 1 veins and connected tendrils together are 10.3 mm long (6.2 and 2.8 mm individually, with a ~1 mm gap, see [Fig. 4](#) and [EA-1](#)) with a greatest width of 3.3 mm and typical depth of ~1 mm. Sample 2 also contains two discontinuous veins of similar proportions and structure. The vein structure in Sample 2 has greatest dimensions of 6.2 × 2.9 mm with a variable depth of 0.4 to 1.5 mm.

[Rubin \(2003\)](#) observed that silicate peninsulas between the metal vein tendrils in Kernouvé possessed a preferred orientation (cf. [Fig. 2](#)). Although we have no quantitative data to support our claim, our 3D observations do not indicate this to be the case. Examined from the perspective of the metal veins, amoeboid protrusions from our metallic veins do not seem to possess a preferred orientation ([Figs. 2, 4 and 5](#)).

We do not know if the metal veins in the AMNH and USNM samples are coplanar or even if they are parallel. Nor do we know how the orientation of metal veins

reported for Kernouvé in a Natural History Museum London (NHM) specimen ([Hutchison et al., 2001](#)) compares to those in our samples. [Hutchison and coworkers \(2001\)](#) indicated that the NHM Kernouvé specimen contains a vein structure that extends for 11 cm, roughly 10 times the longest vein-like structure observed with our 3D techniques. However, the metal veins in our samples have a similar dimension and appearance, and we suspect that they were originally parallel if not also co-planar in the Kernouvé meteorite, like the 30 cm long vein structure seen in the Butsura meteorite and the above mentioned 11 cm veins in Kernouvé ([Hutchison et al., 2001](#)).

3.3. Density, porosity, and physical properties

There have been numerous previous examinations of the physical properties of the Kernouvé H chondrite with which we can compare our results. An early petrography-based determination of the porosity by [Michel-Lévy \(1978\)](#) (also see [Michel-Lévy and Ragot, 1971](#)) found that the macroporosity (defined by them as voids >10 μm in size) was 4 vol.%, and an upper limit of the total porosity of Kernouvé was placed at 9 vol.%. [Britt and Consolmagno \(2003\)](#), citing density measurements from several researchers and a variety of measurements including [Wilkison and Robinson's \(2000\)](#) measured bulk density of 3.65 g/cm³ for a 98 g piece of Kernouvé (Field Museum ME 1484), reported a model porosity of 5.3 vol.%. Using the technique of ideal gas pycnometry and an Archimedean bead method,

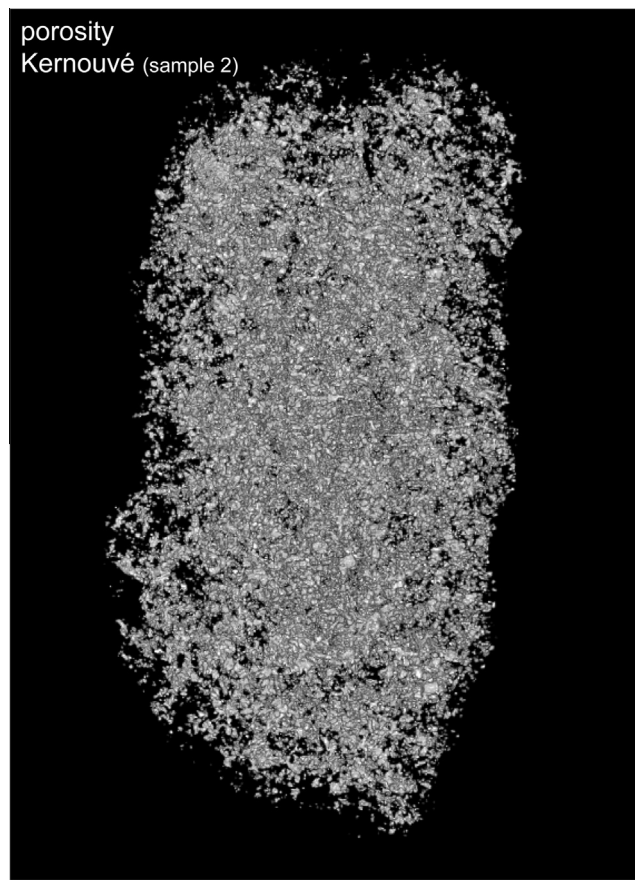


Fig. 6. The structure of porosity in Kernouvé. Porosity in Kernouvé is located in larger intergranular spaces and small voids rather than microcracks. These voids are not interconnected and do not appear to be currently related to the location of metal veins. From top to bottom the sample measures approximately 10.5 mm in total height.

Macke (2010) examined three samples of Kernouvé: two from the Vatican meteorite collection (curation numbers 499 and 1379) and one mass from the AMNH (AMNH 470). Although the subsample of AMNH 470 (different than the subsample used for this study) was too large (148.1 g) for porosity measurement, its bulk density was found to be $3.50 \pm 0.04 \text{ g/cm}^3$. Bulk density measurements of the smaller Vatican samples (29.7 and 18.0 g) respectively yielded 3.40 ± 0.03 and $3.65 \pm 0.07 \text{ g/cm}^3$. Although the bulk densities of the Vatican samples are comparable with H chondrites in general (Consolmagno et al., 2008), Macke's (2010) determined porosities (9.7 ± 1.1 and $2.5 \pm 2.0 \text{ vol.}\%$) were scattered, with a mean of 6.8 vol.%.

Our determined physical properties for Kernouvé samples compare well with previously studied samples. Mean μCT -visible porosity within our larger samples is $4.4 \pm 1.3 \text{ vol.}\%$. This is nearly identical to the 4 vol.% determined by Michel-Lévy (1978), who examined porosity at nearly the same resolution ($\geq \sim 10 \mu\text{m}$) as our μCT work. The slightly lower value of porosity derived from μCT compared to that of the reliable mean 6.8 vol.% pycnometry value (Macke, 2010) is also consistent with previous studies that used both techniques and can be explained by the presence of voids smaller than the imaging resolution (Friedrich et al., 2008b; Sasso et al., 2009). We also examined three

smaller chips at a higher μCT resolution. Results for total porosity at $2.74 \mu\text{m/voxel}$ yielded a higher porosity value of $5.8 \pm 0.9 \text{ vol.}\%$ (Table 1), which compares well with both the Macke measurements and the Britt and Consolmagno (2003) model porosity. We take our 5.8 vol.% measured porosity to be a good value for the total porosity in the Kernouvé chondrite. Our bulk densities also agree well with those previously determined, even for the smaller chips – our determined bulk density ranges from 3.50 to 3.63 g/cm^3 , with the largest sample (Sample 2) giving a value of 3.52 g/cm^3 . Bulk densities vary in the smaller chips with porosity and metal content as expected (Table 1).

Overall, the Kernouvé material used in this study seems representative of the Kernouvé chondrite in general and compares well with typical H chondrite material: the mean porosity and density of H chondrite falls is $7.0 \pm 4.9 \text{ vol.}\%$ and $3.42 \pm 0.18 \text{ g/cm}^3$, respectively (Consolmagno et al., 2008). More important for this study, the structure of the porosity in Kernouvé is significant: porosity is contained in intergranular spaces rather than microcracks (Figs. 1 and 6). This indicates that the meteorite was incompletely compacted, as larger, mm-sized voids would certainly collapse during a significant shock event. Thus the meteorite experienced a very mild late stage uniaxial impact history. Additionally, no relationship exists between the current

location of the porosity and the metal grains or larger metal vein structures.

4. DISCUSSION

4.1. Summary of previous studies of Kernouvé

Before we begin consideration of our newly acquired data, we will first examine some previous studies that have considered the Kernouvé H6 S1 chondrite, which has been examined by numerous investigators. We summarize the evidence and general conclusions below.

Michel-Lévy (1978, 1981) and a coworker (Michel-Lévy and Ragot, 1971) suggested that metallic veins in Kernouvé formed as a linear accumulation of metal due to a tectonic disturbance. These workers suggested that Kernouvé “recrystallized” (which can be interpreted as “metamorphosed”) largely undisturbed after a 4.54 Ga event recorded as an ^{40}Ar – ^{39}Ar age (Turner et al., 1978), which resulted in well-preserved fission tracks (Pellas and Storzer, 1981). Michel-Lévy (1982) found observable porosity in petrographic thin section, but only small degrees of inferred permeability (interconnectedness). This was taken as an indication that Kernouvé experienced some compression and recrystallization coincident with or after the metamorphic heating event.

Hutson (1989) noted that several sections of Kernouvé contain elongate metal masses, which she interpreted as a partially obliterated metal vein. She cited the work of Michel-Lévy (above) as an indicator of partially annealed shock features.

Rubin (1992, 1994, 2003, 2004) included observations of Kernouvé and inferred from various petrographic indicators that the meteorite experienced an episode of shock loading followed by annealing, although Kernouvé has a shock stage of S1. These indicators include the presence of large (up to cm-sized) metal veins that are the subject of this study, chromite veinlets, and chromite-plagioclase assemblages (Rubin, 2003, 2004). Rubin additionally cited previous works including that of Hutson (1989) and Turner et al. (1978) to conclude that metal veins in Kernouvé are a manifestation of an early impact process.

Hutchison et al. (2001) synthesized evidence for the pre-metamorphic origin for the veins in Kernouvé including that of Michel-Lévy (above) and an uneventful metallographic cooling history (Yang et al., 1997). They also cited the work of Leroux et al. (1996) who argued that a pre-metamorphic shock event injected micron-sized metal and sulfide material into fractures in silicate crystals.

Collectively, and based on a variety of evidence, these independent workers have produced a consistent history of the Kernouvé H chondrite. These previous hand sample, petrographic, two-dimensional (2D) microscopy, and radiochronologic studies agree that Kernouvé experienced an early tectonic event, generally interpreted as an impact, which produced the large metallic veins as well as other possible petrographic indicators. This event was very early in the history of the rock, probably prior to or coincident with thermal metamorphism on the H chondrite parent body. Today, Kernouvé appears mildly-shocked, possessing an S1 shock stage. Given these prior observations, we will use our newly collected data to examine the nature and intensity of the shock event that produced the metal veins in Kernouvé. Prior and new observations of Kernouvé and their implications are summarized in Table 2.

4.2. Insights into Kernouvé from 3D petrography

From the above traditional petrographic observations, we have seen that Kernouvé appears mildly shocked, but has indications of a complex history. While our own thorough petrographic analyses have additionally confirmed an S1 shock stage, our 3D observations also allow us to examine the complexity of Kernouvé’s history in more detail.

4.2.1. Porosity and compaction

The 5.8 vol.% porosity contained in Kernouvé is not exceptionally high – ordinary chondrites with porosities as great as ~20 vol.% are known – but we have seen that the structure of the porosity is primarily contained within intergranular pores rather than the microcracks that are indicative of higher degrees of shock loading and compaction (see Figs. 1 and 2; cf. Friedrich and Rivers, 2013). If

Table 2
Observations and corresponding inferences for Kernouvé.

Observation	References	Inference
(1) S1 character	This work, 1–4	Olivine weakly strained
(2) Early Ar and W isotopic closure, Pu fission tracks	5–7	No late shock heating
(3) Low preferred orientation of metal	This work	No late shock compaction
(4) ~5% Porosity	This work, 8–12	Some shock compaction
(5) Intergranular porosity	This work, 8 and 9	Little late, strong shock compaction
(6) Little microcracking in silicates	This work	Microcracks annealed or never produced
(7) Coarse metal veins present, with offsets	This work, 1–5, 13–15	Probably created by shear, possibly by high-temperature deformation
(8) Coarse metal has tendrils, complex 3D shape	This work	Metamorphic growth of metal

Reference key: 1 – Rubin (1992), 2 – Rubin (1994), 3 – Rubin (2003), 4 – Rubin (2004), 5 – Turner et al. (1978), 6 – Pellas and Storzer (1981), 7 – Trieloff et al. (2003), 8 – Michel-Lévy and Ragot (1971), 9 – Michel-Lévy (1978), 10 – Wilkison and Robinson (2000), 11 – Britt and Consolmagno (2003), 12 – Macke (2010), 13 – Michel-Lévy (1981), 14 – Hutson (1989) and 15 – Hutchison et al. (2001).

we take 20–30 vol.% porosity (a minimum value at best) to be a pre-metamorphic value for typical ordinary chondritic porosity, we can surmise that at least 70–80% of the original porosity in Kernouvé has been removed due to compaction and possibly metamorphic recrystallization (Henke et al., 2012). Impacts are the most efficient method of removing porosity from an initial state (Hirata et al., 2008) in chondrites, as lithostatic overpressure alone in a ~100 km body is insufficient to generate the force necessary for efficient compression.

If Kernouvé was compacted, which the quantity of porosity suggests, this is not manifested as a preferred orientation of the ductile metal grains in the material. Fig. 3 demonstrates that the metal grains in Kernouvé possess among the lowest degree of collective orientation of any chondrite. While collective orientation of metal grains correlates well with degree of apparent shock loading (Fig. 3), we note that it is primarily an indicator of late stage shock-related compaction.

Given these constraints, we put forward that Kernouvé did experience some compaction, probably in the form of one or more impacts, but given the low shock stage, porosity structure, and lack of collective degree of metal grain orientation, this must have happened early in the history of the rock. Post-compaction thermal annealing reduced the apparent petrographic shock indicators to those seen in an S1 classification and also obliterated any preferred

orientation of typical H chondrite sized metal grains in the material. We propose that the thermal event that produced the heat necessary for the annealing was the same heat required for thermal metamorphism of Kernouvé to petrographic type 6, and given the very old ^{39}Ar – ^{40}Ar age found by Turner et al. (1978), ^{26}Al is the most likely source, but some minor quantity of heat would have been generated by the impact event itself. This scenario correlates well with those of all previous investigations of Kernouvé mentioned above (Section 4.1).

4.2.2. Coarse metal veins

The metal vein structures found in Kernouvé (Figs. 2, 4 and 5, EA-1 and EA-2) can be regarded as abnormally large metal grains with a complex overall shape. The overall metal abundance in the vein-containing samples is not especially high and does not indicate a significant concentration of metal (Table 1), unlike what is seen in Portales Valley (Ruzicka et al., 2005). Fig. 7 shows both the vein metal and all other metal grains found in Sample 1 of Kernouvé. The metal veins appear to be local concentrations of native H chondrite Fe–Ni metal (Fig. 7, EA-3). Larger central parts of the interconnected “vein” grains are generally oblate to planar, with numerous tendrils extending from the sides and also connecting the major portions of the vein structure (Figs. 4 and 5). Interestingly, the metal veins are not generally associated with sulfide. It is

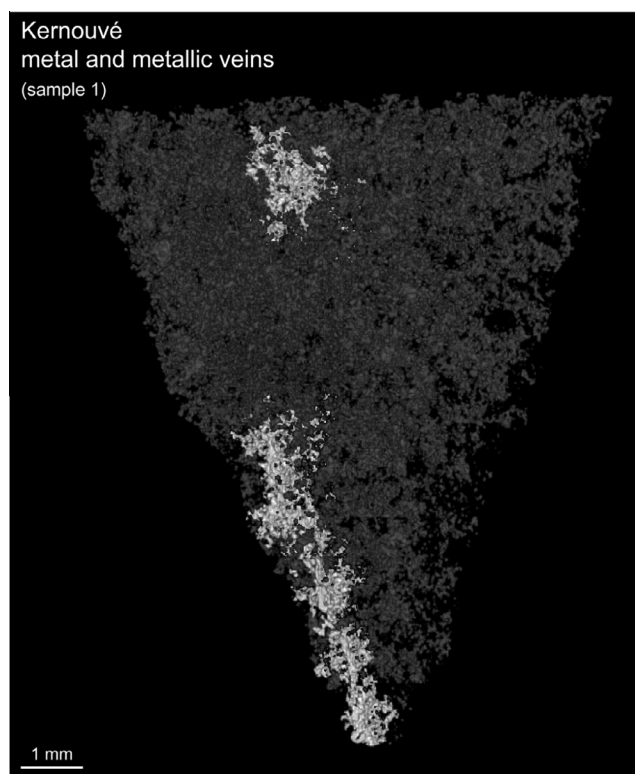


Fig. 7. A 3D representation of both vein (light grey) and typical metal grains (dark grey) in Sample 1 of Kernouvé (corresponds to EA-3). This view is at the same orientation as the 90° view of Fig. 4. The vein structure appears to be a local concentration of metal within the chondrite. The high concentration of typical metal grains in an H chondrite may, at first glance, make them appear to be interconnected, but further inspection (EA-3) reveals their isolated nature. Metal veins were distinguished by their large size and completely connected structure.

conceivable that metal and troilite were present together in the veins originally, but that these became separated, during immiscible separation or during crystallization. If the metal veins possessed a less complex linear structure, a later stage impact origin would be viable, but the complexity of the shape belies a recent history: thermal metamorphism has likely played a role in the attaching of tendrils and imparting a coarse structure onto the veins.

Sufficient time was available for creating the complex shape of the grains, and growth during metamorphism is known to increase the size of metal grains in ordinary chondrites. We have no metallographic cooling rates for the veins within Kernouvé; however, we see no reason to reject an assumption that the veins followed the same cooling trajectory as the smaller metal grains. This assumption is supported by the absence of brecciation textures, and we see no evidence for infiltration of metal following metamorphism (also see [Reisener and Goldstein, 2003](#)). Metal grains in Kernouvé have been heated above the kamacite–taenite transition of about 700 °C ([Holland-Duffield et al., 1991](#)). During slow cooling, kamacite grows within the taenite and the rate of cooling can be derived from the composition of the metallic grains. Using this, researchers have determined metallographic cooling rates in Kernouvé to be ~17 °C/Ma ([Holland-Duffield et al., 1991](#); [Yang et al., 1997](#); [Reisener and Goldstein, 2003](#)). Following cooling below 400 °C, the metal grains were not heated above the kamacite–taenite transition: Kernouvé had a very uneventful life following the early compaction and vein formation event(s). Thus, a pre-metamorphic or syn-metamorphic origin for both the veins and compaction structure seems likely. Finally, we note that the compaction and vein formation events may have been simultaneous or temporally separated: our data are unable to distinguish between the two possibilities. Both scenarios are possible.

4.3. Shear as a metal vein formation mechanism in Kernouvé

Mechanisms for the concentration of metal in chondritic materials can be split into two categories: (1) partial melting of a Fe,Ni–FeS eutectic during heating with movement of liquid into fractures and (2) shear deformation involving ductile accumulation of metal grains. The former can involve several means of melting the metal–troilite mixture, including either shock-related or non-collisional (static) heat sources, and this can act on a variety of scales.

The first possibility, invoking a static heat source, was proposed for creating the cm-scale metal and troilite vein structures in the Monument Draw acapulcoite by [McCoy et al. \(1996\)](#) and the similar scale metal-rich areas in Portales Valley H7 chondrite ([Pinault et al., 1999](#)). However, this mechanism should produce a metal–troilite eutectic mixture which would be reflected in the resulting mineralogy, but this clearly is not observed in Kernouvé. Veins in Kernouvé cannot be explained this way without further separation of metal from troilite, but supersolidus immiscibility or crystallization could, in principle, segregate Fe–Ni metal and FeS. However, there is no evidence that Kernouvé was metamorphosed beyond petrographic type 6,

whereas the meteorite examples given above experienced higher temperatures.

Collisional heating with the injection of Fe, Ni–FeS liquids into silicate cracks at high temperatures generally acts on smaller scales (µm) than is seen in the vein structures of Kernouvé. [Leroux et al. \(1996\)](#) argued that a pre-metamorphic shock event within Kernouvé caused injection of a metal and sulfide rich liquid into an open fracture network within silicate crystals. This was used by [Hutchison et al. \(2001\)](#) as a formation mechanism for the metal veins in Kernouvé. However, the [Leroux et al. \(1996\)](#) study focused on tiny (sub µm to µm sized) Fe,Ni–FeS materials purportedly squeezed into fractures within the silicates. The work of [Leroux et al. \(1996\)](#) was not necessarily meant to indicate an origin for the larger metallic vein structures found in Kernouvé, but nonetheless it may be applicable. It is known that shock at higher temperatures can form larger-scale metal structures. [Ruzicka et al. \(2005\)](#) surmised an ambient temperature of about 900 °C for Portales Valley at the time of shock. Metal nucleated in the vein from Fe,Ni–FeS liquids, and continued growing, pushing troilite into the adjacent host. This mechanism could result in contiguous troilite in the meteorite, which is not seen in Kernouvé.

Although the coarse metal veins in Kernouvé are composed entirely of metal, unlike the much smaller metal–troilite “injections”, we cannot completely rule out a similar injection origin for the coarse veins followed by metal and troilite separation due to immiscibility or during crystallization. Given especially that the porosity and physical structure of Kernouvé prior to the formation of the metal veins is unknown, it is conceivable that squeezing of hot metal-rich material could yield the structures seen in Kernouvé. However, the squeezing of metal into fractures mandates that a fracture (or high permeability porosity) network exists: if no prior fracture network exists for the metal to flow into, vein formation by this mechanism would be impossible. If blocks of indurated material were present within a primordial H chondrite parent, another mechanism, perhaps acting in conjunction with squeezing for vein-like metal grain formation may be more efficient than squeezing alone: shear. Such a mechanism would additionally account for the roughly planar shapes (and offsets) of metal veins seen in Kernouvé ([Figs. 4 and 5, EA-1 and EA-2](#)).

Shear deformation with accompanying accumulation is a means of concentrating Fe–Ni metal and sulfide into veins. The enhanced ductility of these phases allows for vein structures to be formed as either a solid or liquid. [Bruhn et al. \(2000\)](#), [Nakamura et al. \(2000\)](#), [van der Bogert et al. \(2003\)](#), [Groebner and Kohlstedt \(2006\)](#), and [Rushmer et al. \(2000, 2005\)](#) have shown the feasibility of impact and shear deformation as a mechanism for vein formation at scales ranging from µm to mm. Metal concentration via shear would be enhanced at high temperatures during deformation. [Nakamura et al. \(2000\)](#) found the largest concentration (~2 mm area) of metal and sulfide by shock deformation at 600 °C in an experimental CV chondrite charge.

We propose a shear mechanism for the initial concentration of vein metal seen in Kernouvé. Semi-consolidated

blocks of porous material were disturbed by an impact causing a physical concentration of metallic phases upon their faces due to lateral motion between the blocks. In this scenario, the enhanced ductility of metal compared to silicate is considered to be a key property that enabled metal to concentrate in vein-like structures. Such ductility would be greatly enhanced if the target were already warm. Thus, the coarse metal vein formation would have been facilitated by a shock event while metamorphism was occurring. Besides shearing, a more uniaxial compression or squeezing is needed to account for the porosity seen in Kernouvé. Such uniaxial compression could have occurred during the same deformation event that resulted in shear or it could have occurred in a different event.

4.4. Constraints on the deformation history of Kernouvé

We here summarize and expand on the discussion presented above, with Table 2 listing eight pertinent observations and inferences that bear on the thermal and deformation history of Kernouvé.

The S1 character, early isotopic closure, low preferred orientation of typical metal grains, and presence of large intergranular voids in the meteorite (observations or obs. 1,2,3,5—Table 2) are all consistent with Kernouvé having experienced little late shock deformation. On the other hand, the presence of moderate (~5 vol.%) indigenous porosity, absence of significant numbers of microcracks, presence of coarse metal veins, and complex 3D shape of the veins (obs. 4, 6, 7, 8 – Table 2) are all consistent with early deformation that was followed by annealing, reflecting either pre-metamorphic or syn-metamorphic deformation. We suggest that syn-metamorphic deformation can best explain the coarse veins, consistent with the results of experiments that show that metal mobilizes readily into intergranular veins when deformation occurs at elevated temperatures (Nakamura et al., 2000; Rushmer et al., 2000, 2005; Groebner and Kohlstedt, 2006). Either pre- or syn-metamorphic deformation can also explain the S1 character of the Kernouvé, if optical evidence for strain in olivine was reduced by annealing or high temperature effects.

Metamorphic redistribution of metal can explain both the complex 3D shape of metal as well as the destruction of any preferred orientation of typical-sized metal grains (obs. 8 and 3, Table 2). Such redistribution could potentially also relate to the presence of large intergranular void spaces (obs. 5, Table 2), if metal migrated from smaller to coarser grains to leave voids behind. Although movement of metal out of voids is consistent with the sizes of the intergranular pores, which are similar to typical smaller metal grains, we have not discerned any spatial relationship between voids and coarse metal to indicate movement of metal from one to the other.

The deformation that resulted in the veins and the moderate porosity (obs. 7 and 4, Table 2) could reflect the same shock event. This shock event was sufficiently strong to reduce porosity, but not so strong as to reduce porosity much below the ~5 vol.% value found in the meteorite. Based on shock experiments (Hirata et al., 2008; Nakamura et al.,

2000), shock events with peak pressures of only ~2–3 GPa (corresponding to shock stage S1) are able to significantly reduce porosity, but to obtain ~5 vol.% porosity from an initially porous material requires a peak pressure of ~21–22 GPa (shock stage S3/S4 transition, Stöfler et al., 1991). Thus one might infer a shock pressure of ~21–22 GPa for Kernouvé. This value is uncertain as it assumes no change in porosity during annealing, experimental conditions that match those experienced by Kernouvé, and target materials that deform in the same way. Although the first assumption is probably valid, considering that metamorphism probably occurred under low-pressure conditions, the second and third assumptions may not be. In particular, if temperature of deformation was higher than used in the experiments (room temperature to ~600 °C), such as at a peak metamorphic temperature of 800–900 °C, one might obtain more compaction for a particular peak pressure, as grains would be more ductile and likely to flow. Also, multiple weak impacts could result in relatively more compaction. Finally, the target materials used in the experiments (the metal-poor, matrix-rich Allende CV chondrite) may not have responded in the same way as a metal-rich, matrix-poor ordinary chondrite. These considerations suggest that the veins and porosity in Kernouvé could have formed by one or more shock events that involved ≤ 21 GPa peak shock pressure, but better estimates of the pressure value could be obtained by repeating shock experiments using an H chondrite charge over a larger temperature range.

4.5. Implications for shear-produced metal veins in Kernouvé

Shear deformation is believed to be an important aspect for differentiation of planetesimals (Bruhn et al., 2000; Rushmer et al., 2000, 2005; Groebner and Kohlstedt, 2006; Hustoft and Kohlstedt, 2006; Rushmer and Petford, 2011). It has been demonstrated that shear deformation, such as may be produced via planetary impacts, can produce interconnected networks of metal within silicates much like those seen within the metallic vein structures of Kernouvé (Bruhn et al., 2000; Groebner and Kohlstedt, 2006). We also note that in the Bruhn et al. (2000) and Groebner and Kohlstedt (2006) experiments, metal segregated into melt-enriched zones completely in the plastic flow regime without the fracturing of silicate. These observations are similar to what we propose for the formation metal veins in Kernouvé. The formation of these networks increases the permeability of metal melts within silicate matrices and allows for core formation within the time frames mandated by isotopic constraints. Our studies of Kernouvé provide further evidence for shear deformation on chondritic parent bodies and suggest that collision-induced interconnected metal networks were forming at an early stage in planetesimals.

The total physical scale of the shear-produced metal veins produced by this mechanism is uncertain. In our samples, the total scale is in the cm range, but the effect (production of multiple mm-wide concentrations of metal) was probably an order of magnitude larger. Metal concentration areas stretch for at least decimeters. We have no

spatial provenance for the metal vein structures between our AMNH and USNM samples, which were likely derived from adjacent areas of the same rock. We also have no provenance for the metal structures in other samples of Kernouvé where metal veins have been shown to exist including the UCLA LC884 or NHM specimens (see Hutchison et al., 2001; Rubin, 2003, 2004). Although it would be informative for our hypothesis to show that metal veins among these samples were coplanar, we do not have this information. We do note, however, that similar veins in the 29 kg Butsura H chondrite (Hutchison et al., 2001) that would be large enough to encompass large samples, and at different institutions (see Section 3.2). Our proposed shear-based mechanism, operating on the cobble to boulder scale, is consistent with observed metal veins found in these hand samples and this mechanism may have been operating at a time when planetary differentiation was occurring in other planetesimals.

5. CONCLUSIONS

Kernouvé is an H6 chondrite that has experienced a very small degree of late stage shock loading. However, there is evidence for early impact deformation followed by annealing: the moderate 5.8 vol.% porosity implies some shock compaction, and the porosity is in the form of intergranular voids rather than cracks, which indicates any cracking that may have existed in the relatively brittle silicate grains was annealed. We estimate that 70–80% of the primordial porosity in Kernouvé was removed by impact-related compaction. However, we found no collective orientation of metal grains, so high metamorphic temperatures erased any common orientation of metal grains due to compaction. The impact conditions, including possibly a high ambient temperature, allowed metal to localize on cm-scales within the parent body, creating metallic vein-like structures which have survived largely unaffected since their creation and cooling. Given the above evidence and shape of these structures, we propose that they can be explained as a pre- or syn-metamorphic shock-induced process, which we infer was primarily shear deformation coupled with some uniaxial compression for the removal of porosity. The peak pressure of the vein-forming, porosity-reducing shock event was likely ≤ 21 GPa. The complexity of shape, including numerous tendrils expanding from the primary structure, of the veins in Kernouvé is due to the additional coalescence of metal after the shear event. The metal veins in Kernouvé record evidence for shock-induced metal mobilization processes that were potentially important for enabling planetesimal differentiation.

ACKNOWLEDGMENTS

This study was supported by NASA's Origin of Solar Systems (OSS) Program grant NNX10AH336 (PI AR, Co-I JMF). J.M.F. would additionally like to thank the Fund for Astrophysical Research for assistance in the acquisition of computer equipment used for portions of this study. Portions of this work were performed at GeoSoilEnviroCARS (Sector 13), Advanced Photon Source (APS), Argonne National Laboratory. GeoSoilEnviroCARS is supported

by the National Science Foundation – Earth Sciences (EAR-0622171) and Department of Energy – Geosciences (DE-FG02-94ER14466). Use of the Advanced Photon Source was supported by the U.S. Department of Energy, Office of Science, Office of Basic Energy Sciences, under Contract No. DE-AC02-06CH11357. The authors thank Drs. D. Hezel and D.L. Kohlstedt for constructive and helpful reviews. Dr. W.U. Reimold is thanked for thorough and swift editorial handling.

APPENDIX A. SUPPLEMENTARY DATA

Supplementary data associated with this article can be found, in the online version, at <http://dx.doi.org/10.1016/j.gca.2013.01.009>.

REFERENCES

- Beitz E., Blum J., Mathieu R., Pack A. and Hezel D. C. (2013) Experimental investigation of the nebular formation of chondrule rims and the formation of chondrite parent bodies. *Geochim. Cosmochim. Acta* **116**, 41–51.
- Britt D. T. and Consolmagno G. J. (2003) Stony meteorite porosities and densities: a review of the data through 2001. *Meteorit. Planet. Sci.* **38**, 1161–1180.
- Bruhn D., Groebner N. and Kohlstedt D. L. (2000) An interconnected network of core-forming melts produced by shear deformation. *Nature* **403**, 883–886.
- Consolmagno G. J., Britt D. T. and Macke R. J. (2008) The significance of meteorite density and porosity. *Chem. Erde* **68**, 1–29.
- Ebel D. S., Weisberg M. K., Hertz J. and Campbell A. J. (2008) Shape, metal abundance, chemistry and origin of chondrules in the Renazzo (CR) chondrite. *Meteorit. Planet. Sci.* **43**, 1725–1740.
- Friedrich J. M., Wignarajah D. P., Chaudhary S., Rivers M. L., Nehru C. E. and Ebel D. S. (2008a) Three-dimensional petrography of metal phases in equilibrated L chondrites – effects of shock loading and dynamic compaction. *Earth Planet. Sci. Lett.* **275**, 172–180.
- Friedrich J. M., Macke R. J., Wignarajah D. P., Rivers M. L., Britt D. T. and Ebel D. S. (2008b) Pore size distribution in an uncompacted equilibrated ordinary chondrite. *Planet. Space Sci.* **56**, 895–900.
- Friedrich J. M. and Rivers M. L. (2013) Three-dimensional imaging of ordinary chondrite microporosity at 2.6 micrometer resolution. *Geochim. Cosmochim. Acta* **116**, 63–70.
- Groebner N. and Kohlstedt D. L. (2006) Deformation-induced metal melt networks in silicates: implications for core-mantle interactions in planetary bodies. *Earth Planet. Sci. Lett.* **245**, 571–580.
- Henke S., Gail H.-P., Trieloff M., Schwarz W. H. and Kleine T. (2012) Thermal evolution and sintering of chondritic planetesimals. *Astron. Astrophys.* **537**, A45.
- Hirata N., Kurita K. and Sekine T. (2008) Simulation experiments for shocked primitive materials in the Solar System. *Phys. Earth Planet. Inter.* **174**, 227–241.
- Holland-Duffield C. E., Williams D. B. and Goldstein J. I. (1991) The structure and composition of metal particles in two type 6 ordinary chondrites. *Meteoritics* **26**, 97–103.
- Hustoft J. W. and Kohlstedt D. L. (2006) Metal-silicate segregation in deforming dunitic rocks. *Geochem. Geophys. Geosyst.* **7**, Q02001. <http://dx.doi.org/10.1029/2005GC001048>.
- Hutchison R., Williams I. P. and Russell S. S. (2001) Theories of planetary formation: constraints from the study of meteorites. *Philos. Trans. R. Soc. London A* **359**, 2077–2093.

- Hutson M. (1989) Shock effects in H-group chondrites. *Lunar Planet. Sci.* **XX**, 436–437, abstract.
- Jamsja N. and Ruzicka A. (2010) Shock and thermal history of NWA 4859, an annealed impact-melt breccia of LL-chondrite parentage containing unusual igneous features and pentlandite. *Meteorit. Planet. Sci.* **45**, 828–849.
- Jarosewich E. (1990) Chemical analyses of meteorites – A compilation of stony and iron meteorite analyses. *Meteoritics* **25**, 323–337.
- Ketchum R. A. (2005) Computational methods for quantitative analysis of three dimensional features in geological specimens. *Geosphere* **1**, 32–41.
- Kleine T., Touboul M., van Orman J. A., Bourdon B., Maden C., Mezger K. and Halliday A. N. (2008) Hf W thermochronometry: closure temperature and constraints on the accretion and cooling history of the H chondrite parent body. *Earth Planet. Sci. Lett.* **270**, 106–118.
- Leroux H., Doukhan J.-C. and Guyot F. (1996) An analytical electron microscopy (AEM) investigation of opaque inclusions in some type 6 ordinary chondrites. *Meteorit. Planet. Sci.* **31**, 767–776.
- Macke R. J. (2010) Survey of meteorite physical properties: density, porosity, and magnetic susceptibility. Ph. D. thesis, University of Central Florida.
- McCoy T. J., Keil K., Clayton R. N., Mayeda T. K., Bogard D. D., Garrison D. H., Huss G. R., Hutcheon I. D. and Wieler R. (1996) A petrologic, chemical, and isotopic study of monument draw and comparison with other acapulcoites: evidence for formation by incipient partial melting. *Geochim. Cosmochim. Acta* **60**, 2681–2708.
- Michel-Lévy M. C. (1978) Estimation del la Porosite de quelques chondrites par analyse d'images de leurs sections polies. *Meteoritics* **13**, 305–309.
- Michel-Lévy M. C. (1981) Some clues to the history of the H-group chondrites. *Earth Planet. Sci. Lett.* **54**, 67–80.
- Michel-Lévy M. C. and Ragot J. P. (1971) La texture des chondrites observée en plaques minces par fluorescence ultraviolette. *Meteoritics* **6**, 217–224.
- Nakamura T., Tomeoka K., Takaoka K., Sekine T. and Takeda H. (2000) Impact-induced textural changes of CV carbonaceous chondrites: experimental reproduction. *Icarus* **146**, 289–300.
- Pellas P. and Storzer D. (1981) ²⁴⁴Pu fission track thermometry and its application to stony meteorites. *Proc. R. Soc. London A* **374**, 253–270.
- Pinault L. J., Scott E. R. D., Bogard D. D. and Keil K. (1999) Extraordinary properties of the metal-veined, H6 Portales Valley chondrite: evidence for internal heating versus shock-melting origins. In *30th Lunar and Planetary Science Conference*. CD-ROM. #2048 (abstr.)
- Reisener R. J. and Goldstein J. I. (2003) Ordinary chondrite metallography: Part 2. Formation of zoned and unzoned metal particles in relatively unshocked H, L, and LL chondrites. *Meteorit. Planet. Sci.* **38**, 1679–1696.
- Rubin A. E. (1992) A shock-metamorphic model for silicate darkening and compositionally variable plagioclase in CK and ordinary chondrites. *Geochim. Cosmochim. Acta* **56**, 1705–1714.
- Rubin A. E. (1994) Metallic copper in ordinary chondrites. *Meteoritics* **29**, 93–98.
- Rubin A. E. (2003) Chromite-plagioclase assemblages as a new shock indicator: implications for the shock and thermal histories of ordinary chondrites. *Geochim. Cosmochim. Acta* **67**, 2695–2709.
- Rubin A. E. (2004) Postshock annealing and postannealing shock in equilibrated ordinary chondrites: implications for the thermal and shock histories of chondritic asteroids. *Geochim. Cosmochim. Acta* **68**, 673–689.
- Rushmer T. and Petford N. (2011) Microsegregation rates of liquid Fe–Ni–S metal in natural silicate–metal systems: a combined experimental and numerical study. *Geochem. Geophys. Geosyst.* **12**, Q03014. <http://dx.doi.org/10.1029/2010GC003413>.
- Rushmer T., Minarek W. G. and Taylor G. J. (2000) Physical processes of core formation. In *Origin of Earth and Moon* (eds. R. M. Canup and K. Righter). The University of Arizona Press, Tucson, pp. 227–245.
- Rushmer T., Petford N., Humayan M. and Campbell A. J. (2005) Fe liquid segregation in deforming planetesimals: coupling core-forming compositions with transport phenomena. *Earth Planet. Sci. Lett.* **239**, 185–202.
- Ruzicka A., Killgore M., Mittlefehldt D. W. and Fries M. D. (2005) Portales valley: petrology of a metallic-melt meteorite breccia. *Meteorit. Planet. Sci.* **40**, 261–295.
- Sasso M. R., Macke R. J., Boesenberg J. S., Britt D. T., Rivers M. L., Ebel D. S. and Friedrich J. M. (2009) Incompletely compacted equilibrated ordinary chondrites. *Meteorit. Planet. Sci.* **44**, 1743–1753.
- Schmitt R. T. (2000) Shock experiments with the H6 chondrite Kernouvé: pressure calibration of microscopic shock effects. *Meteorit. Planet. Sci.* **35**, 545–560.
- Schmitt R. T. and Stöffler D. (1995) Experimental data in support of the 1991 shock classification of chondrites. *Meteoritics* **30**, 574–575.
- Stöffler D., Keil K. and Scott E. R. D. (1991) Shock metamorphism of ordinary chondrites. *Geochim. Cosmochim. Acta* **55**, 3845–3867.
- Trieloff M., Jessberger E. K., Herrwerth I., Hopp J., Fiéni C., Ghélis M., Bourrot-Denise M. and Pellas P. (2003) Structure and thermal history of the H-chondrite parent asteroid revealed by thermochronometry. *Nature* **422**, 502–506.
- Turner G., Enright M. C. and Cadogan P. H. (1978) The early history of chondrite parent bodies inferred from ⁴⁰Ar–³⁹Ar ages. *Proc. Lunar Planet. Sci. Conf. 9th*. pp. 989–1025.
- van der Bogert C. H., Schultz P. H. and Spray J. G. (2003) Impact induced frictional melting in ordinary chondrites: a mechanism for deformation, darkening, and vein formation. *Meteorit. Planet. Sci.* **38**, 1521–1531.
- Wilkison S. L. and Robinson M. S. (2000) Bulk density of ordinary chondrite meteorites and implications for asteroidal internal structure. *Meteorit. Planet. Sci.* **35**, 1203–1213.
- Woodcock N. H. (1977) Specification of fabric shapes using an eigenvalue method. *Geo. Soc. Am. Bull.* **88**, 1231–1236.
- Woodcock N. H. and Naylor M. A. (1983) Randomness testing in three-dimensional orientation data. *J. Struct. Geo.* **5**, 539–548.
- Yang C.-W., Williams D. B. and Goldstein J. I. (1997) A new empirical cooling rate indicator for meteorites based on the cloudy zone of the metallic phases. *Meteorit. Planet. Sci.* **32**, 423–429.